RESEARCH PAPER

Intranasal Solid Lipid Nanoparticles of Efavirenz in Thermosensitive Gel for Enhanced Brain Targeting: Formulation, Optimization, and Evaluation

Adilakshmi Challa[1], M. Mohan Varma[2], P. Shailaja[3]

[1]Research Scholar, Department of Pharmaceutics, Shri Vishnu College of Pharmacy, Bhimavaram, AP, India.
Email: adipharma222@gmail.com

[2]Professor, Department of Pharmaceutics, Shri Vishnu College of Pharmacy, Bhimavaram, AP, India.
Email: mohan@svcp.edu.in (Corresponding Author)

[3]Asso. Professor, Department of Pharmaceutics, A.U College of Pharmacy, Andhra University, Vishakhapatnam, AP, India

ABSTRACT

Background: Efavirenz (EFV), a first-line NNRTI, shows limited oral bioavailability due to low solubility, first-pass metabolism, high protein binding, and efflux, and it poorly penetrates the blood–brain barrier, leaving the CNS as an HIV reservoir.

Objective: To develop and optimize EFV-loaded solid lipid nanoparticles (SLNs) for intranasal, nose-to-brain delivery, and to incorporate them into a thermosensitive in-situ gel to enhance brain targeting and bioavailability.

Methods: A systematic workflow covered excipient screening, process/formulation optimization (high-pressure homogenization; 3^2 factorial design: drug:lipid ratio and surfactant concentration as factors), and characterization of the optimized SLN dispersion (particle size, PDI, zeta potential, EE), followed by integration into a poloxamer-based in-situ gel (with Carbopol 934P as mucoadhesive). UV methods at 247 nm in 50% methanol:water and methanolic PBS pH 6.4 supported assay, EE, and release. Ex-vivo release used Franz cells with goat nasal mucosa; release kinetics were modeled.

Results: Optimized SLNs exhibited mean size 108.5 nm, PDI 0.172, zeta potential −21.2 mV, and entrapment 64.9%, indicating a narrow distribution and good colloidal stability. A thermoreversible gel using poloxamer 188:407 = 1:2 with Carbopol 934P 0.4% w/v gelled at ~34 °C in <1 min, aligning with nasal mucosal temperature and supporting residence time. Intranasally administered EFV-SLN gel achieved a brain-to-plasma ratio of 12.61% vs 0.104% for oral standard (≈120-fold brain-targeting enhancement) and relative bioavailability 80.12-fold vs oral drug powder. Long-term stability (12 months) was established at 5 ± 3 °C and 25 ± 2 °C/60 ± 5% RH per ICH guidance.

Conclusion: Intranasal EFV-SLN in thermosensitive in-situ gel significantly enhances brain delivery and systemic absorption versus oral EFV, supporting its potential to address CNS HIV reservoirs.

Keywords: Efavirenz; solid lipid nanoparticles; intranasal; nose-to-brain delivery; in-situ gel; poloxamer; brain targeting; bioavailability.

How to cite this article: Challa A, Varma MM, Shailaja P. Intranasal Solid Lipid Nanoparticles of Efavirenz in Thermosensitive Gel for Enhanced Brain Targeting: Formulation, Optimization, and Evaluation. Int J Drug Deliv Technol. 2026;16(50s): 1-19. DOI: 10.25258/ijddt.16.50s.1

Source of support: Nil.

Conflict of interest: None

Introduction

Eradication of HIV remains constrained by sanctuary sites such as the central nervous system (CNS), where suboptimal drug penetration fosters viral persistence and neurocognitive complications. Despite effective plasma viral suppression, conventional oral antiretrovirals often fail to achieve therapeutic levels in the brain due to the blood–brain barrier and first-pass/efflux liabilities.[1]

Efavirenz (EFV) is a recommended first-line NNRTI (HAART) but displays BCS Class II behavior (low aqueous solubility, high lipophilicity), extensive first-pass metabolism, and high protein binding, collectively yielding ~40–45% bioavailability and limited CNS exposure.[2] These features motivate alternative delivery strategies that both bypass hepatic first-pass and exploit direct olfactory/trigeminal pathways for nose-to-brain transport.[3]

Solid lipid nanoparticles (SLNs) are attractive carriers for EFV: their lipidic core can improve permeability, protect drug from enzymatic degradation, and limit efflux, while nanoscale size favors mucosal uptake. An intranasal, thermoresponsive in-situ gel can further enhance residence time and reduce anterior leakage, improving deposition and transport toward the olfactory region.[4]

The main aim of this study is to design and optimize EFV-loaded SLNs for intranasal delivery and embed them in a thermosensitive in-situ gel to enhance brain targeting and overall bioavailability.

The Objectives of proposed research work is (i) Screen and select safe lipids/surfactants and a robust SLN

process; (ii) apply design of experiments to optimize critical variables (drug:lipid ratio, surfactant concentration, and homogenization conditions) for desirable particle size/PDI/EE; (iii) formulate a poloxamer-based in-situ gel with mucoadhesive support to extend nasal residence; (iv) develop/validate UV analytical methods for EE and release; (v) compare in-vitro and ex-vivo performance (goat nasal mucosa) and evaluate in-vivo brain/plasma disposition relative to oral EFV.

The Hypothesis of the study is EFV-SLNs administered intranasally will (a) increase absorption due to small particle size and permeation-enhancing excipients, (b) protect EFV from enzymatic degradation and first-pass metabolism, (c) reduce efflux via pluronic surfactants, and (d) deliver EFV directly to the CNS, improving brain targeting at lower doses.

2. Materials and Methods

2.1 Materials

Efavirenz (EFV) was obtained as a gift sample from Sun Pharma Ltd., Hyderabad, India. Delavirdine (DEV) was used as an additional NNRTI for comparative purposes. Lipids screened included glyceryl monostearate, glyceryl distearate, glyceryl tripalmitate (tripalmitin), and glyceryl palmitostearate (Sigma Aldrich, Bangalore). Surfactants comprised poloxamers (Pluronic F68/Poloxamer 188, Pluronic F127/Poloxamer 407, Pluronic P85/Poloxamer 245) and polysorbates (Tween 20, 60, 80). Gelling agents included chitosan and Carbopol 934P (S.D. Fine Chemicals Ltd., Mumbai). Thermosensitive polymers poloxamer 188 and poloxamer 407 were also sourced from S.D. Fine Chemicals. Solvents (methanol, acetonitrile, isopropyl alcohol) and buffer salts were analytical grade. Potassium bromide (FTIR grade) was procured from Fischer Scientific, Mumbai.

2.2 Identification of Drug

EFV identity was confirmed through preliminary compendial tests and FTIR spectroscopy. Appearance, solubility (in water and methanol), and melting point were compared with reported data. FTIR spectra were obtained (Bruker Alpha-FTIR) by KBr disc method, scanning 4000–400 cm^{-1}, and compared with reference spectra to confirm functional groups.[5,6]

2.3 Analytical Methods

A UV spectrophotometric method was developed and validated (Shimadzu UV-1800, λmax = 247 nm). Calibration curves were constructed in (i) 50% v/v methanol:water and (ii) methanolic phosphate-buffered saline (PBS, pH 6.4, 40% v/v), selected to reflect nasal mucosal pH while ensuring sink conditions. Calibration was linear (2–12 µg/ml; $R^2 \approx$ 0.999), and regression equations were used to quantify EFV in entrapment, release, and stability samples.[7]

2.4 Preformulation Studies

2.4.1 Lipid Screening

EFV solubility was assessed in lipids heated to 5 °C above their melting points using a water bath shaker. Tripalmitin exhibited the highest solubilizing capacity (~135 mg/g lipid), significantly greater than other candidates ($p < 0.05$), and was selected for formulation.[8]

2.4.2 Surfactant Screening

Nanoparticles were prepared with tripalmitin and individual surfactants. Particle size, polydispersity index (PDI), and entrapment efficiency (EE) were evaluated by dynamic light scattering (Malvern Zetasizer Nano ZS). Poloxamer 188 yielded the smallest particle size (568.4 ± 7.5 nm), lowest PDI (0.584), and highest EE (24.9%), thus selected for further optimization.[9,10]

2.4.3 Drug–Excipient Compatibility

FTIR spectra of EFV, tripalmitin, and poloxamer 188 mixtures confirmed the retention of EFV's characteristic peaks with no significant spectral shifts, indicating compatibility[11].

2.5 Formulation Development

2.5.1 Formulation Technique

Two methods were compared: solvent evaporation and high-pressure homogenization (HPH). HPH produced smaller particles (~378.3 ± 8.5 nm) with superior EE (~65.8%) versus solvent evaporation (~469.7 nm; EE ~40.2%) ($p < 0.01$). Moreover, HPH avoids organic solvents and is scalable. Thus, HPH (hot homogenization) was selected[12].

2.5.2 Optimization of Process Variables

Critical steps (stirring, homogenization, and sonication) were optimized:

- **Stirring:** 10,000 rpm for 15 min produced ~350 nm particles with PDI ~0.39.
- **HPH:** A 3^2 factorial design (Design Expert v12) investigated homogenization pressure and cycle number as factors, targeting minimal particle size and PDI.
- **Sonication:** Optimized for dispersion stabilization without aggregation[13].

2.5.3 Optimization of Formulation Variables

A 3^2 factorial design (factors: drug: lipid ratio, surfactant concentration) was applied. Responses: particle size, PDI, and EE[14]. Response surface methodology and ANOVA identified an optimal region yielding ~108.5 nm particles, PDI 0.172, EE 64.9%, and zeta potential −21.2 mV.

2.6 Development of Thermosensitive In-Situ Gel

Poloxamers 188 and 407 were screened for gelling ability. The optimized ratio (1:2) provided gelation at ~34 °C within 1 min. Carbopol 934P (0.4% w/v) was added for mucoadhesion. EFV-SLN dispersion was

incorporated, producing a transparent, easily flowing solution at room temperature that gelled rapidly at nasal physiological temperature[15].

2.7 Evaluation

2.7.1 Physicochemical Characterization

Optimized EFV-SLNs were evaluated for particle size/PDI/zeta potential (Zetasizer Nano ZS), morphology (TEM), and entrapment efficiency (centrifugation + UV assay at 247 nm)[16]. Gel formulations were tested for gelation temperature/time, pH, viscosity, transmittance, spreadability, and mucoadhesive strength[17-19].

2.7.2 In-Vitro Release

Drug release was studied by dialysis membrane method using methanolic PBS pH 6.4 (50% v/v) as receptor medium. Aliquots withdrawn over 24 h were analyzed spectrophotometrically. Release data were fitted to kinetic models (zero-order, first-order, Higuchi, Korsmeyer–Peppas)[20,21].

2.7.3 Ex-Vivo Absorption

Freshly excised goat nasal mucosa was mounted in Franz diffusion cells. EFV-SLN gel, plain EFV suspension, and controls were applied to donor compartments. Drug permeation was quantified in receptor fluid. Histopathological evaluation (H&E staining) confirmed no mucosal damage compared to negative controls[22-24].

2.7.4 In-Vivo Studies

Adult male Wistar rats were divided into test (intranasal EFV-SLN gel) and standard (oral EFV capsule dispersion) groups (n = 6 each). At 24 h, plasma and brain samples were collected, processed, and analyzed by HPLC (with tenofovir disoproxil fumarate as IS). Pharmacokinetic parameters and brain:plasma ratios were calculated[25,26].

2.7.5 Stability Studies

Optimized EFV-SLN gel was stored at 5 ± 3 °C and 25 ± 2 °C/60 ± 5% RH (ICH conditions). Samples were evaluated up to 12 months for particle size, PDI, zeta potential, and physical appearance[27].

3. Results and Discussion

3.1 Drug Identification

EFV was confirmed as a white crystalline powder, practically insoluble in water but freely soluble in methanol, with a melting point of 139–141 °C. FTIR analysis displayed characteristic peaks for N–H stretching (3318 cm^{-1}), C≡C (2150 cm^{-1}), C=O ester (1748 cm^{-1}), and C=O amide (1632 cm^{-1}), consistent with reported spectra represented in table 1 and figure 1. These findings confirmed the identity and purity of the sample.

3.2 Analytical Method Validation

Calibration curves for EFV in (i) methanol:water (50% v/v) and (ii) methanolic PBS (pH 6.4, 40% v/v) were linear across 2–12 µg/ml, with correlation coefficients R^2 = 0.999. The λmax was determined as 247 nm. These validated UV spectrophotometric methods were applied for entrapment efficiency, drug release, and stability testing. The calibration graphs represented in figure 2 (a) and 2 (b).

3.3 Design of Experiments

Quality Target Product Profile (QTPP) and Critical Quality Attributes (CQAs) were defined, with emphasis on particle size (minimal), PDI (<0.2), entrapment efficiency (maximized), and zeta potential (≥ ±20 mV for stability). Preliminary experiments confirmed excipient compatibility, and factorial design (3^2) was used to optimize process and formulation variables.

3.4 Preformulation Studies

3.4.1 Lipid Selection

EFV showed highest solubility in glyceryl tripalmitate (tripalmitin: ~135 mg/g), significantly higher than glyceryl monostearate (~62 mg/g) or glyceryl distearate (~42 mg/g). Tripalmitin was therefore selected for SLN formulation, aligning with literature reporting its safety (GRAS) and suitability for lipid nanoparticles.

3.4.2 Surfactant Selection

Tripalmitin-based nanoparticles stabilized with different surfactants were compared. Poloxamer 188 (Pluronic F68) produced the smallest particle size (568.4 ± 7.5 nm) with favorable PDI (0.584) and highest EE (24.9%) compared with other surfactants. Its non-ionic, steric stabilization properties and GRAS status further supported its selection.

3.4.3 Compatibility

FTIR spectra of EFV + tripalmitin + poloxamer 188 mixtures showed no significant peak shifts, confirming compatibility and absence of interactions.

3.5 Formulation Technique

Two preparation techniques were evaluated: solvent evaporation and high-pressure homogenization (HPH). HPH yielded significantly smaller particles (378.3 ± 8.5 nm) and higher EE (65.8%) than solvent evaporation (469.7 nm; 40.2% EE) ($p < 0.01$). Moreover, HPH avoids toxic organic solvents and supports scale-up, so was selected.

3.6 Optimization of Variables

3.6.1 Process Variables

Stirring at 10,000 rpm for 15 min reduced particle size to ~350 nm with acceptable PDI. Factorial optimization of homogenization (pressure, cycles) confirmed that higher pressure and cycles reduced size

but excessive processing increased PDI, likely due to aggregation. Sonication optimized dispersion stability.

3.6.2 Formulation Variables

Factorial design varying drug:lipid ratio and surfactant concentration identified optimal conditions yielding particles of 108.5 nm, PDI 0.172, EE 64.9%, and zeta potential −21.2 mV. These values align with desirable CQAs for stable, monodisperse SLNs.

3.7 Thermosensitive In-Situ Gel

Poloxamer-based gels were screened for gelation behavior. The optimized system—poloxamer 188:407 (1:2) with Carbopol 934P 0.4% w/v—gelled within 1 min at ~34 °C, closely matching nasal cavity temperature. This system supported prolonged nasal residence and mucoadhesion, while maintaining pH ~6.0, appropriate for nasal mucosa.

3.8 *In-Vitro* and *Ex-Vivo* Release

EFV release from SLNs showed sustained behavior compared to plain drug suspension. Release followed zero-order kinetics ($R^2 = 0.9983$), indicating diffusion-controlled release. Ex-vivo permeation studies across goat nasal mucosa demonstrated significantly higher drug permeation from EFV-SLN gel than from plain EFV, confirming enhanced absorption potential. Histopathology confirmed no tissue damage or irritation.

3.9 *In-Vivo* Pharmacokinetics

In rats, intranasal EFV-SLN gel achieved a brain:plasma ratio of 12.61%, compared with only 0.104% for orally administered EFV powder—demonstrating a ~120-fold improvement in brain targeting. Relative bioavailability was enhanced ~80-fold. These results support the hypothesis of nose-to-brain transport, bypassing first-pass metabolism and efflux.

3.10 Stability Studies

Stability testing under ICH conditions (5 ± 3 °C and 25 ± 2 °C/60 ± 5% RH for 12 months) confirmed no significant changes in particle size, PDI, zeta potential, or appearance, establishing the robustness of the formulation.

4. Summary and Conclusions

4.1 Summary of Work

The present study aimed to overcome the limitations of oral Efavirenz (EFV) low solubility, extensive first-pass metabolism, efflux, and poor CNS penetration—by designing solid lipid nanoparticles (SLNs) for intranasal nose-to-brain delivery. Preformulation studies identified tripalmitin as the optimal lipid and poloxamer 188 as the preferred surfactant. High-pressure homogenization, optimized by factorial design, produced EFV-SLNs with particle size 108.5 nm, PDI 0.172, zeta potential −21.2 mV, and entrapment efficiency 64.9%.

To prolong nasal residence, the optimized SLNs were incorporated into a thermosensitive in-situ gel (poloxamer 188:407 at 1:2 + Carbopol 934P 0.4% w/v), which gelled at 34 °C within 1 min and demonstrated suitable viscosity, mucoadhesion, and pH. In-vitro release followed zero-order kinetics ($R^2 = 0.9983$), and ex-vivo permeation across goat nasal mucosa confirmed enhanced drug transport without mucosal damage.

In-vivo pharmacokinetics in rats revealed a brain:plasma ratio of 12.61% for intranasal EFV-SLN gel versus 0.104% for oral EFV—corresponding to a 120-fold enhancement in brain targeting. Relative bioavailability was increased ~80-fold compared to oral EFV powder. Stability studies under ICH conditions confirmed long-term stability up to 12 months.

Collectively, these results demonstrate that intranasal EFV-SLN in a thermosensitive gel provides a robust, safe, and effective approach for improving brain delivery of EFV.

4.2 Conclusion

EFV-loaded SLNs, optimized by design of experiments and delivered intranasally in a poloxamer-based in-situ gel, achieved substantial improvements in brain targeting and systemic bioavailability compared to oral EFV. This delivery system bypasses first-pass metabolism, reduces efflux, and enhances patient acceptability. With further clinical validation, it could represent a breakthrough strategy in targeting CNS HIV reservoirs and improving antiretroviral therapy outcomes.

4.3 Future Scope

Combination formulations of EFV with other antiretrovirals in SLN-gels to enhance therapeutic efficacy and minimize resistance. Mechanistic evaluations of EFV distribution within specific CNS subregions, to better understand reservoir targeting. Clinical translation involving pharmacokinetic, pharmacodynamic, and safety studies in human subjects. The nose-to-brain nanocarrier strategy holds promise not only for HIV but also for CNS infections and neurodegenerative diseases.

References

1. Das Neves J, Amiji MM, Bahia MF, Sarmento B. Nanotechnology-based systems for the treatment and prevention of HIV/AIDS. *Adv Drug Deliv Rev*. 2010;62(4–5):458-477.
2. Blasi P, Giovagnoli S, Schoubben A, Ricci M, Rossi C. Solid lipid nanoparticles for

targeted brain drug delivery. *Adv Drug Deliv Rev*. 2007;59(6):454-477.
3. Gupta U, Jain NK. Non-polymeric nano-carriers in HIV/AIDS drug delivery and targeting. *Adv Drug Deliv Rev*. 2010;62(4–5):478-490.
4. Attama A, Momoh MA, Builders PF. Lipid nanoparticulate drug delivery systems: a revolution in dosage form design and development. In: *Recent Advances in Novel Drug Carrier Systems*. InTechOpen; 2012. p. 107-140.
5. Avachat AM, Parpani SS. Formulation and development of bicontinuous nanostructured liquid crystalline particles of efavirenz. *Colloids Surf B Biointerfaces*. 2015;126:87-97.
6. Eskandari S, Varshosaz J, Minaiyan M, Tabbakhian M. Brain delivery of valproic acid via intranasal administration of nanostructured lipid carriers: in vivo pharmacodynamic studies using rat electroshock model. *Int J Nanomedicine*. 2011;6:363-371.
7. Abbas Z. Mucoadhesive in situ gels as nasal drug delivery systems: an overview. *Drug Deliv Transl Res*. 2012;7(3):168-180.
8. AbdelMouez M, Zaki NM, Mansour S, Geneidi AS. Bioavailability enhancement of verapamil HCl via intranasal chitosan microspheres. *Eur J Pharm Sci*. 2014;51(1):59-66.
9. Gizurarson S. Anatomical and histological factors affecting intranasal drug and vaccine delivery. *Curr Drug Deliv*. 2012;9(6):566-582.
10. FDA. FDA-approved HIV medicines. Available from: https://aidsinfo.nih.gov. Accessed Nov 11, 2016.
11. Müller RH, Shegokar R, Keck CM. 20 years of lipid nanoparticles (SLN & NLC): present state of development & industrial applications. *Curr Drug Discov Technol*. 2011;8(3):207-227.
12. Joshi MD, Müller RH. Lipid nanoparticles for parenteral delivery of actives. *Eur J Pharm Biopharm*. 2009;71(2):161-172.
13. Wissing SA, Kayser O, Müller RH. Solid lipid nanoparticles for parenteral drug delivery. *Adv Drug Deliv Rev*. 2004;56(9):1257-1272.
14. Garbuzenko OB, Mainelis G, Taratula O, Minko T. Inhalation treatment of lung cancer: the influence of composition of nanostructured lipid carriers on distribution of anticancer drugs. *Mol Pharm*. 2014;11(12):3613-3622.
15. Yadav N, Khatak S, Sara UVS. Solid lipid nanoparticles – a review. *Int J Appl Pharm*. 2013;5(2):8-18.
16. Jain S, Jain N, Bhadra D, Tiwary AK. Formulation and evaluation of solid lipid nanoparticles of a water soluble drug: zidovudine. *Chem Pharm Bull (Tokyo)*. 2006;54(5):710-714.
17. Patravale VB, Date AA, Kulkarni RM. Nanosuspensions: a promising drug delivery strategy. *J Pharm Pharmacol*. 2004;56(7):827-840.
18. Pardeike J, Hommoss A, Müller RH. Lipid nanoparticles (SLN, NLC) in cosmetic and pharmaceutical dermal products. *Int J Pharm*. 2009;366(1–2):170-184.
19. Mukherjee S, Ray S, Thakur RS. Solid lipid nanoparticles: a modern formulation approach in drug delivery system. *Indian J Pharm Sci*. 2009;71(4):349-358.
20. Kakkar V, Singh S, Singla D, Kaur IP. Exploring solid lipid nanoparticles to enhance the oral bioavailability of curcumin. *Mol Nutr Food Res*. 2011;55(3):495-503.
21. Garud A, Singh D, Garud N. Solid lipid nanoparticles (SLN): method, characterization and applications. *Int Curr Pharm J*. 2012;1(11):384-393.
22. Mehnert W, Mäder K. Solid lipid nanoparticles: production, characterization and applications. *Adv Drug Deliv Rev*. 2012;64(Suppl):83-101.
23. Doktorovová S, Shegokar R, Rakovsky E, Souto EB, Müller RH. Application of lipid nanoparticles in topical delivery of anti-inflammatory agents: a new perspective for treatment. *Ther Deliv*. 2012;3(7):1007-1022.
24. Paliwal R, Paliwal SR, Kenwat R, Kurmi BD, Sahu MK. Solid lipid nanoparticles: a review on recent perspectives and patents. *Recent Pat Nanotechnol*. 2020;14(1):1-22.
25. Singh S, Dobhal AK, Jain A, Pandit JK. Formulation and evaluation of solid lipid nanoparticles of a poorly soluble drug. *Drug Dev Ind Pharm*. 2010;36(8):922-930.
26. Chalikwar SS, Belgamwar VS, Talele VR, Surana SJ. Solid lipid nanoparticles of tramadol: preparation, characterization and pharmacokinetic studies. *Colloids Surf B Biointerfaces*. 2012;97:150-156.
27. Varshosaz J, Eskandari S, Tabbakhian M. Brain delivery of insulin using chitosan nanoparticles. *J Nanosci Nanotechnol*. 2006;6(9–10):2996-3003.

List of Tables and Figures

Table 1: Major peaks observed and reported for EFV in IR spectra

Observed (cm^{-1})	Reported (cm^{-1})	Inferences
3318.64	3400-3100	N-H Stretching
2150.39	2260-2100	C≡C (Alkyne)
1748.06	1750-1730	C=O Ester
1632.59	1680-1630	C=O Amide
1317.33	1350-1000	C-N
1136.16	1300-1000	C-O

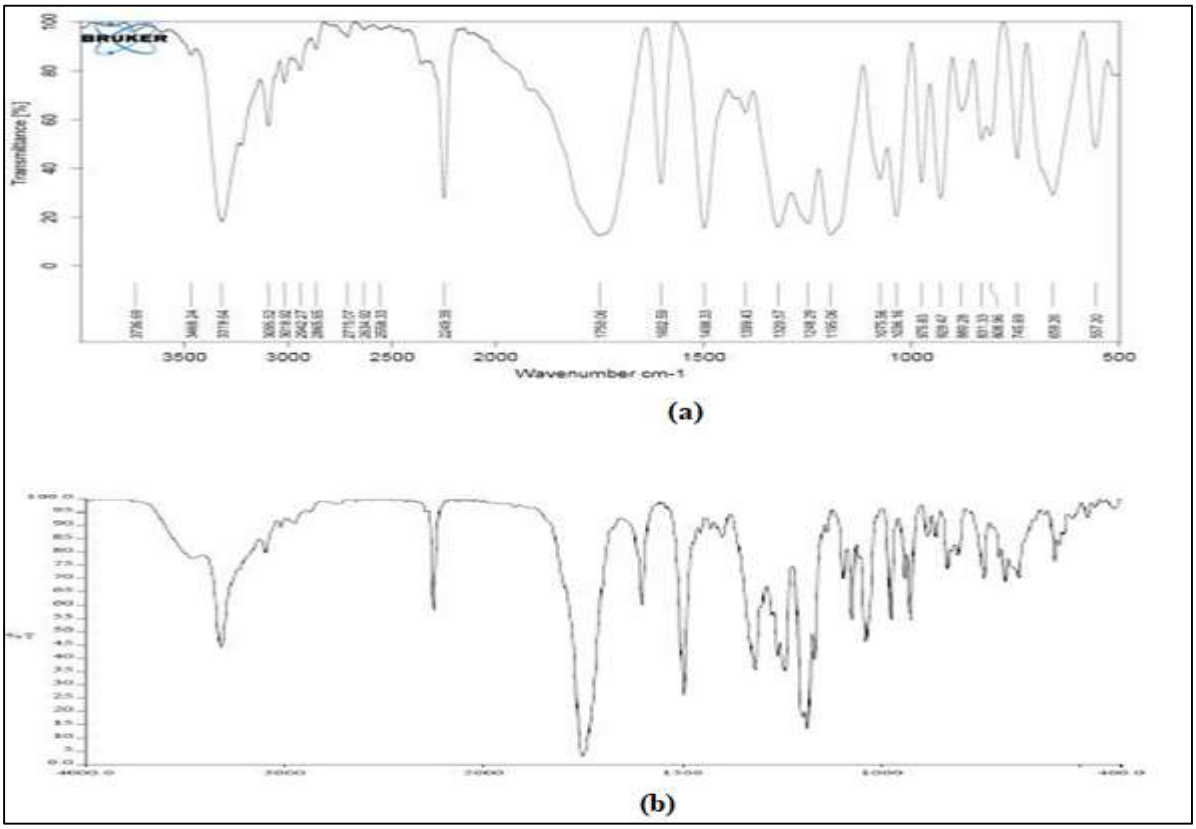

Figure 1: (a) Observed IR spectra of EFV (b) Reported IR spectra of EFV

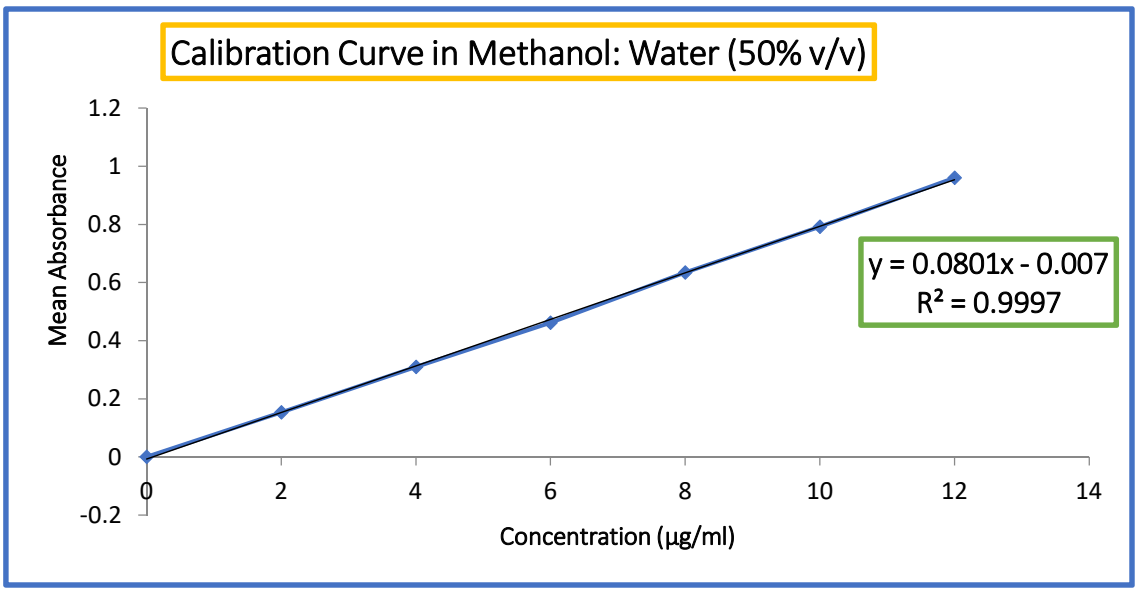

Figure 2 (a): Calibration curve of Efavirenz in methanol and water (50% v/v)

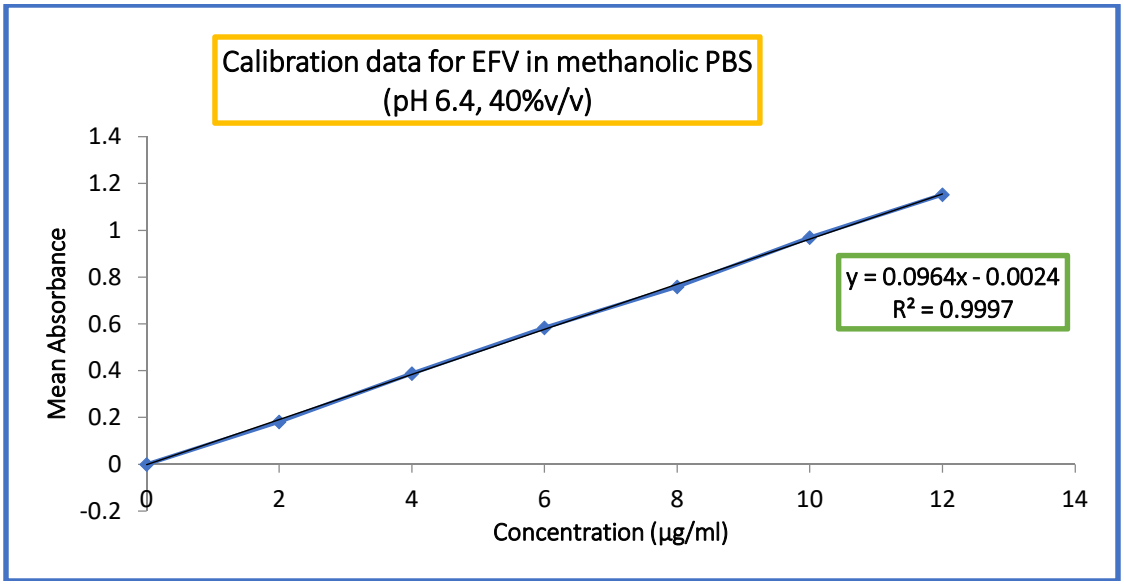

Figure 2 (b) Calibration curve for Efavirenz in 40% methanolic PBS pH 6.4

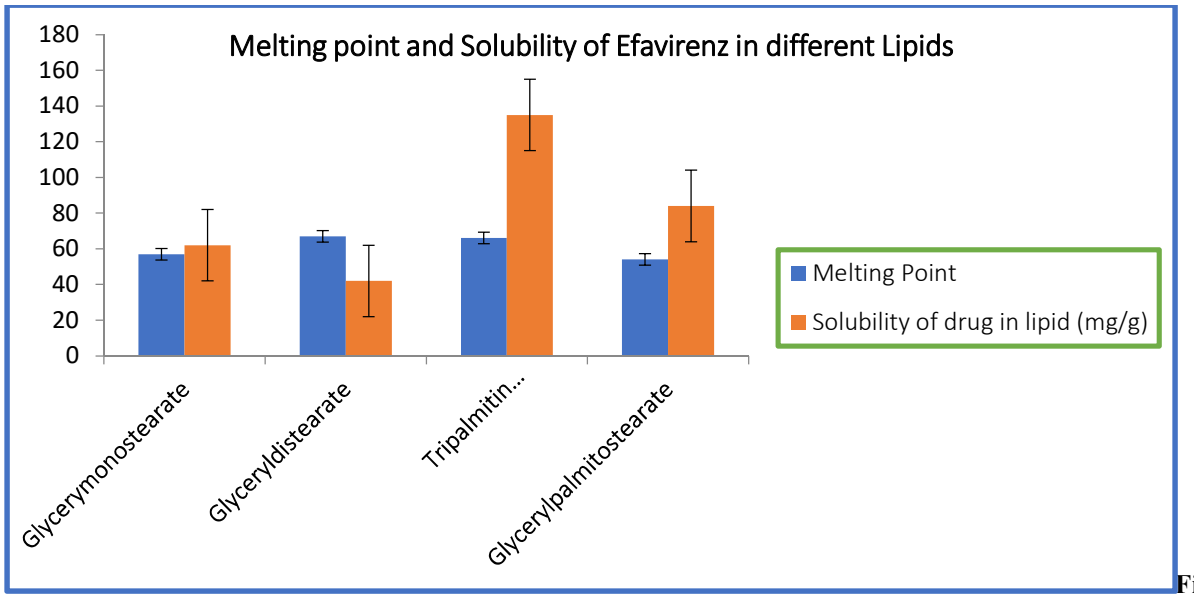

Figure 3: Melting point and Solubility of Efavirenz in different lipids

Table 2: Selection of Surfactant on the basis of Particle size, PDI and Entrapment Efficiency

S. No.	Lipid	Surfactant (1% w/w)	Particle size* (nm)	PDI*	Entrapment Efficiency* (%)
1	**Tripalmitin**	**Poloxamer 188 (PluronicF68)**	**568.4±7.5#**	**0.584±0.3**	**24.95±0.31**
2	Tripalmitin	Poloxamer 407 (PluronicF127)	895.1±7.1	0.463±0.3	17.50±0.41
3	Tripalmitin	Poloxamer245 (PluronicP 85)	629.3±8.3	0.482±0.3	18.51±0.47
4	Tripalmitin	Polysorbate20	689.4±8.7	0.521±0.3	17.43±0.48
5	Tripalmitin	Polysorbate60	622.5+8.8	0.510+0.3	21.14±0.53
6	Tripalmitin	Polysorbate80	600.3±8.5	0.520±0.3	21.33±0.80

*{PDI: Polydispersity Index,*Data expressed as mean±SD (n=3), #indicates statistical significance ($p < 0.05$)}*

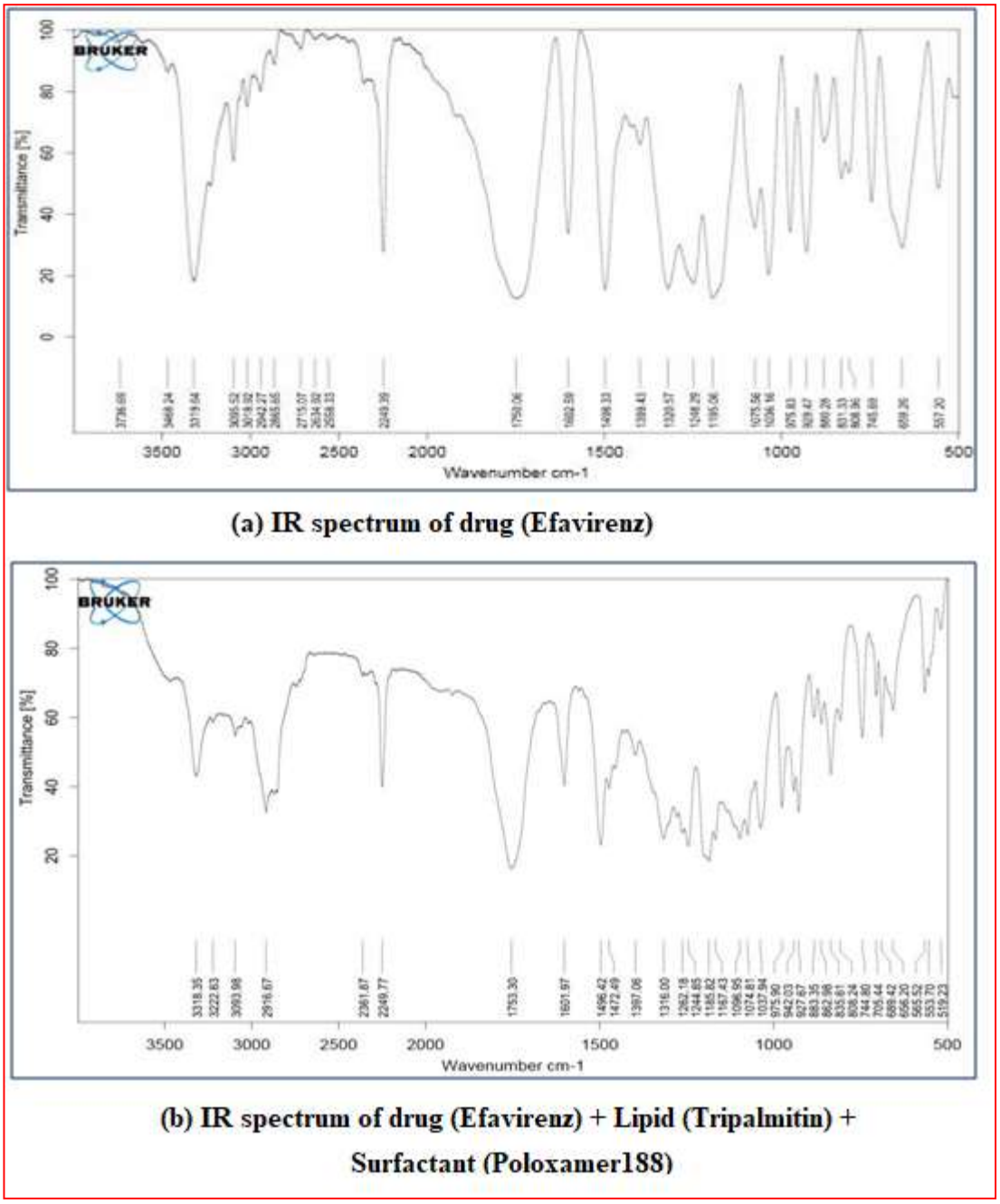

Figure 4: (a) IR spectrum of drug (Efavirenz) (b) IR spectrum of drug (Efavirenz) + Lipid (Tripalmitin) +Surfactant (Poloxamer188)

Table 3: Comparison of formulation techniques on the basis of Particle size, PDI and Entrapment Efficiency

Batch No.	Technique	Particle size* (nm)	PDI*	Entrapment Efficiency* (%)

FT-01	Solvent evaporation	469.7 ±10.4	0.365±0.123	40.24 ±1.3
FT-02	High Pressure Homogenization	**378.3[#] ± 8.5**	**0.375 ±0.112**	**65.78[#]±1.8**

*{PDI: Polydispersity Index, *Data expressed as mean ± SD (n = 3), [#]indicates statistical significance (p<0.01)}*

Table 4: Optimization of stirring speed (rpm) and stirring time (min) on the basis of Particle size and PDI

S. No.	Batch No.	Stirring time (min)	Stirring speed (rpm)	Particle size (nm)	PDI
1	BN-01	10	5000	905.3 ±9.0	0.562 ±0.220
2	BN-02		7500	758.3 ±8.5	0.442 ±0.210
3	BN-03		10000	355.4 ±8.2	0.390 ±0. 192
4	BN-04	**15**	5000	888.6 ±8.4	0.510 ±0.210
5	BN-05		7500	682.0 ±8.0	0.455 ±0.190
6	**BN-06**		**10000**	**350.8±6.4[#]**	**0.390 ±0.180**
7	BN-07	20	5000	856.6 ±6.9	0.442 ±0.122
8	BN-08		7500	503.3 ±6.6	0.552 ±0.114
9	BN-09		10000	318.0 ±6.2	0.631 ±0.114

*{PDI: Polydispersity Index, *Data expressed as mean ± SD (n = 3), [#] indicates statistical significance (p<0.01)}*

Table 5: Optimization of temperature during stirring on the basis of Particle size and PDI

S. No.	Batch No.	Stirring Time (min)	Stirring Speed (rpm)	Temp (^{0}C)	Particle Size (nm)	PDI
1	OT-01	**15**	**10000**	60	454.7 + 4.9	0.523 + 0.133
2	**OT-02**			**70**	**284.2+ 5.0[#]**	**0.252 +0.112**
3	OT-03			80	384.9 + 5.0	0.585 + 0.121

{PDI: Polydispersity Index, *Data expressed as mean ± SD (n = 3), [#]indicates statistical significance (p<0

.01)}

Table 6: Full factorial design with coded and actual values used for optimization of process variables

S. No.	Batch No.	*Coded Values		*Actual Values		Particle size (nm)	PDI
		Pressure (bar)	No. of Cycles	Pressure (bar)	No. of Cycles		
1	OPV-01	-1	-1	500	3	502.0	0.569
2	OPV-02	0	-1	700	3	405.2	0.450
3	OPV-03	1	-1	900	3	310.8	0.422
4	OPV-04	-1	0	500	5	460.7	0.416
5	OPV-05	0	0	700	5	378.3	0.450
6	OPV-06	1	0	900	5	248.1	0.329
7	OPV-07	-1	1	500	7	380.2	0.331
8	OPV-08	0	1	700	7	358.2	0.364
9	OPV-09	1	1	900	7	238.2	0.281
10	OPV-10	0	0	700	5	394.3	0.263
11	OPV-11	0	0	700	5	406.5	0.311
12	OPV-12	0	0	700	5	390.9	0.296
13	OPV-13	0	0	700	5	399.5	0.299

*(Independent variable: Pressure and Number of cycles; Dependent Variable: Particle size and Polydispersity index-PDI)

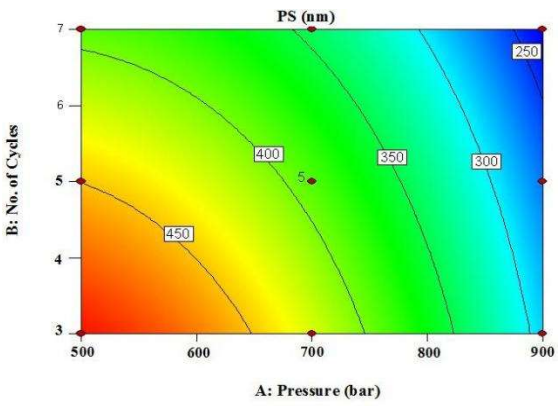

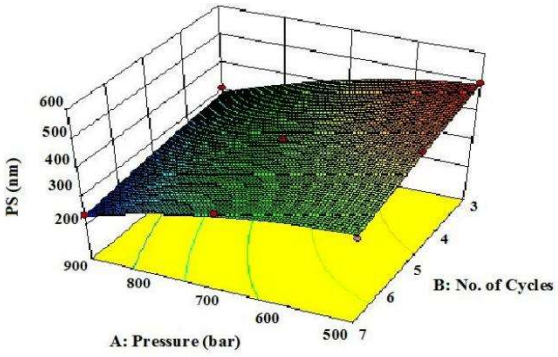

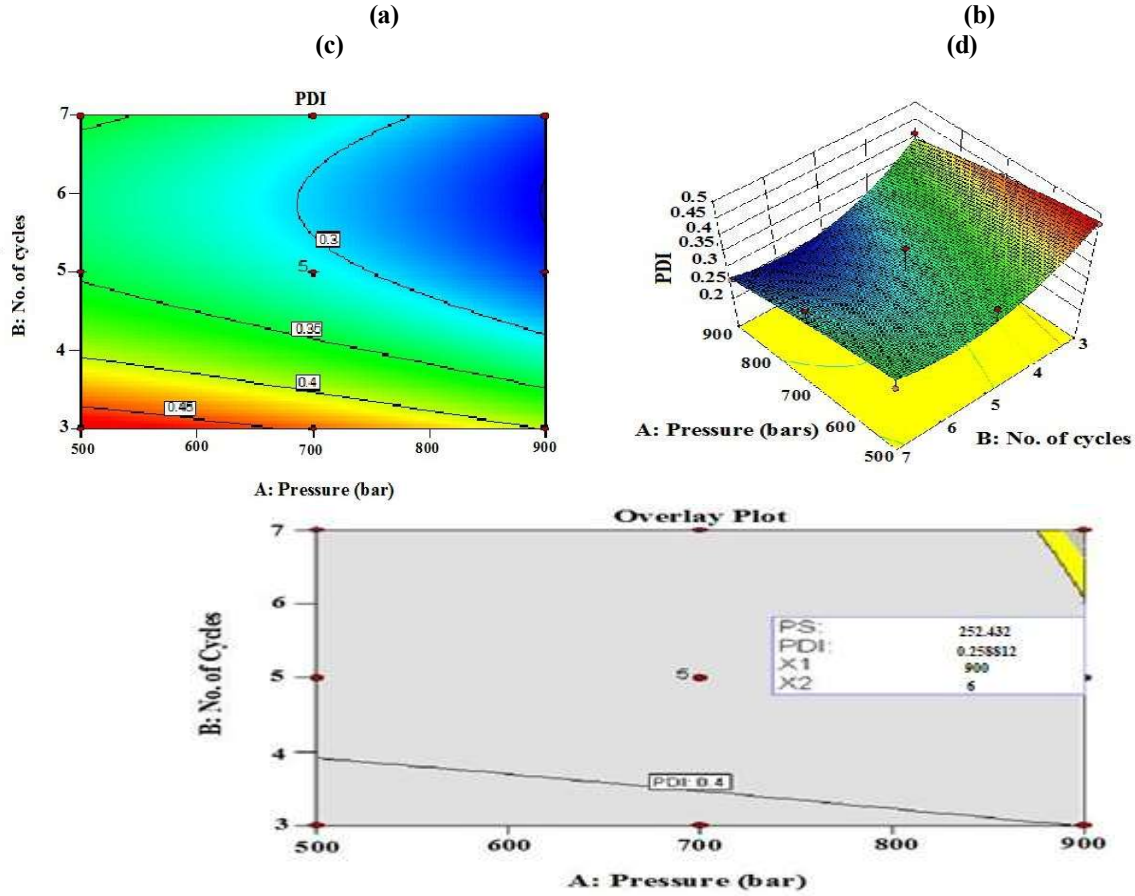

Figure 5: Contour plots, 3D surface plots and overlay plot for process variables (a) Contour plot for particle size (b) 3D Surface plot of Particle Size (c) Contour plot for PDI (d) 3D Surface plot of PDI (e) Overlay plot for optimization

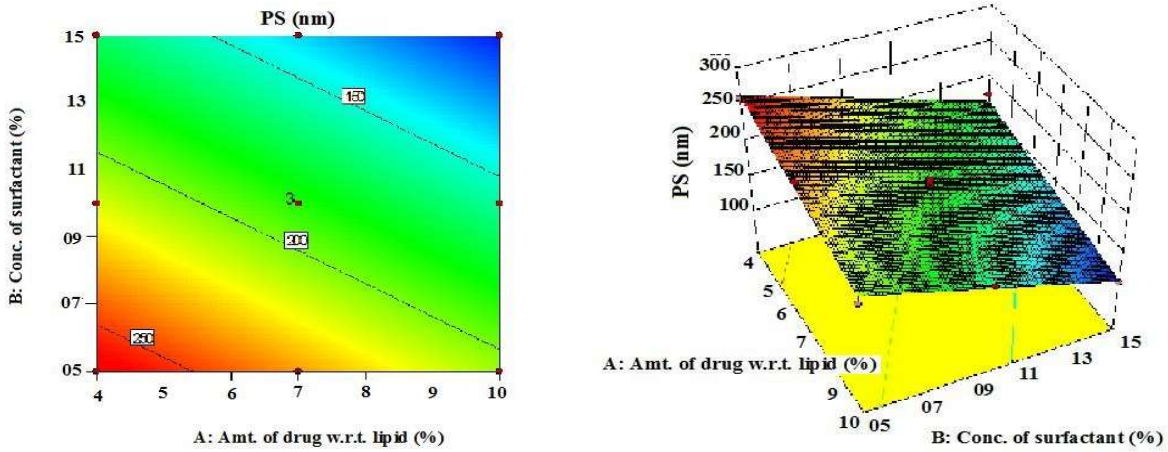

(a) **(b)**

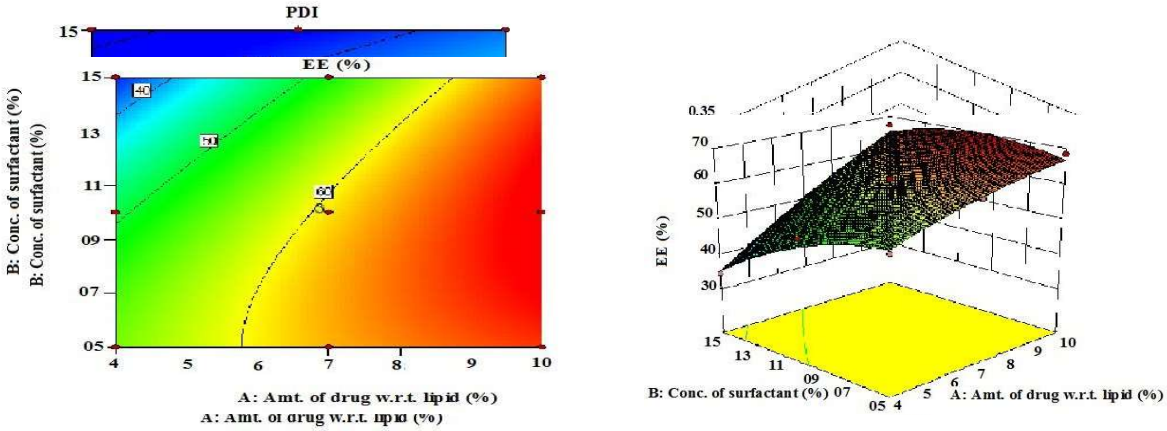

(c) **(d)**

(e) *(f)*

Figure 6: (a) Contour plot for particle size (b) 3D Surface plot of Particle Size (c) Contour plot for PDI (d) 3D Surface plot of PDI (e) Contour plot entrapment efficiency (f) 3D Surface plot of entrapment efficiency

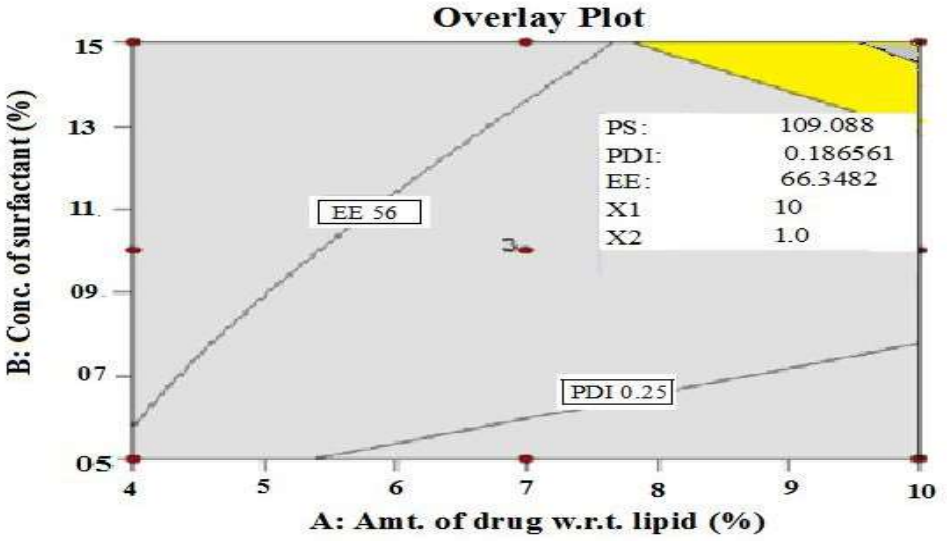

Figure 6 (e): Overlay plot for optimization of formulation variables.

Table 7: Different trials for selection of Gelling/Mucoadhesive agent

S. No.	Trials	Observations
1	100 mg chitosan +10 ml water with Magnetic stirring	Insoluble
2	100 mg chitosan+10 ml warm water (40^0C) with Mag. stirring	Hydrated, lump formation
3	100 mg chitosan+Buffer pH6.4 with Magnetic stirring	Insoluble
4	100 mg chitosan+Buffer pH6.4–heat with Magnetic stirring	Insoluble

5	(100 mg chitosan+5 ml water)+(150 mg Pluronic F68+5 ml water) with Magnetic stirring	Insoluble
6	(100 mg chitosan+5 ml water)+ (150 mg Pluronic F68+5 ml water)-heat with Magnetic stirring	No proper gel
7	100 mg chitosan+10 ml 0.1 M HCl with Mag. stirring	Soluble/gelling
8	Acidic aqueous solution of chitosan+Buffer pH 6.4	Soluble /Slight gelling
9	Carbopol 934P+water with Mag. Stirring	Gel formation
10	**Carbopol 934P+SLNdispersion with Mag. stirring**	**Gel formation**

Table 8: Gelling behavior of SLN dispersion containing thermo responsive polymers at different concentrations of Carbopol 934P

S. No.	Conc. of Carbopol 934P (%w/v)	Temp(^{0}C)	Gelling behavior	
1	0.1	RT (29^{0}C) to 40^{0}C	+	Slight
2	0.2	RT (29^{0}C) to 40^{0}C	++	Moderate
3	0.3	RT (29^{0}C) to 40^{0}C	+++	Considerable
4	**0.4**	**RT (29^{0}C) to 40^{0}C**	**++++**	**Acceptable**
5	0.5	RT (29^{0}C) to 40^{0}C	+++++	High

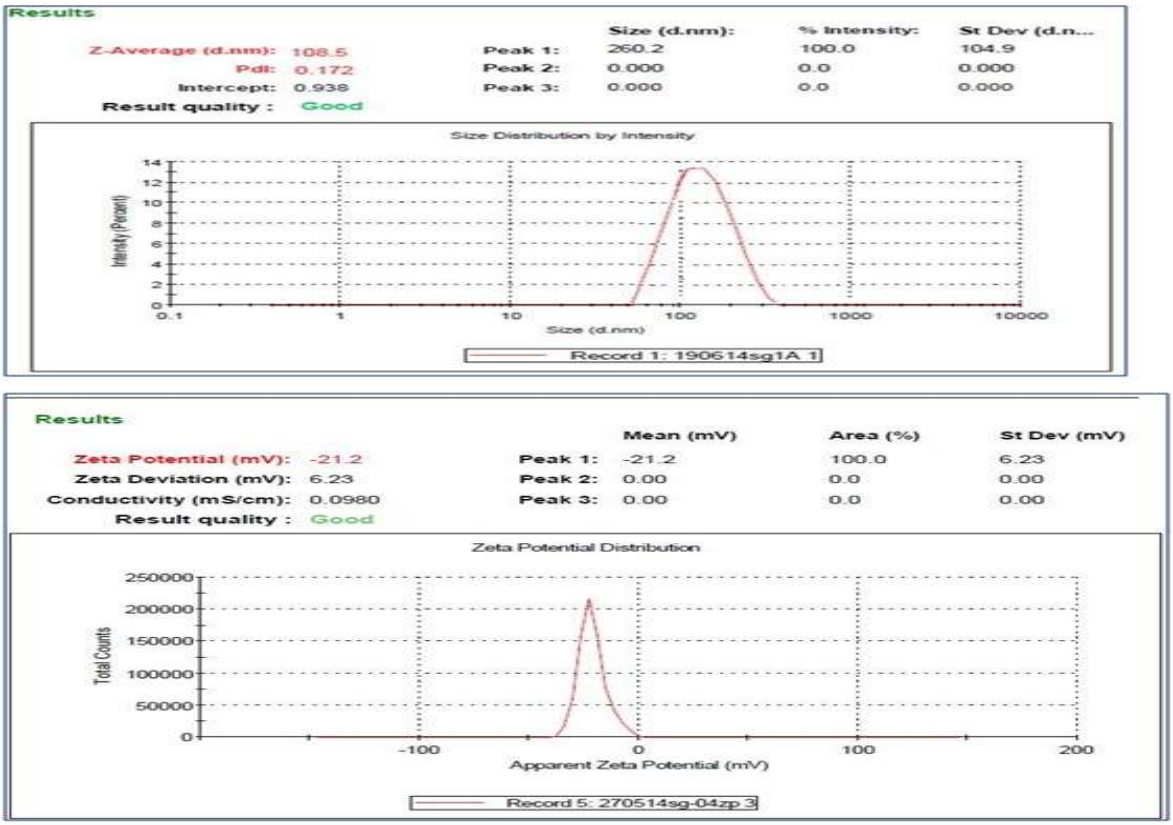

Figure 7: Particle Size distribution and zeta potential distribution of optimized Efavirenz nanoparticles

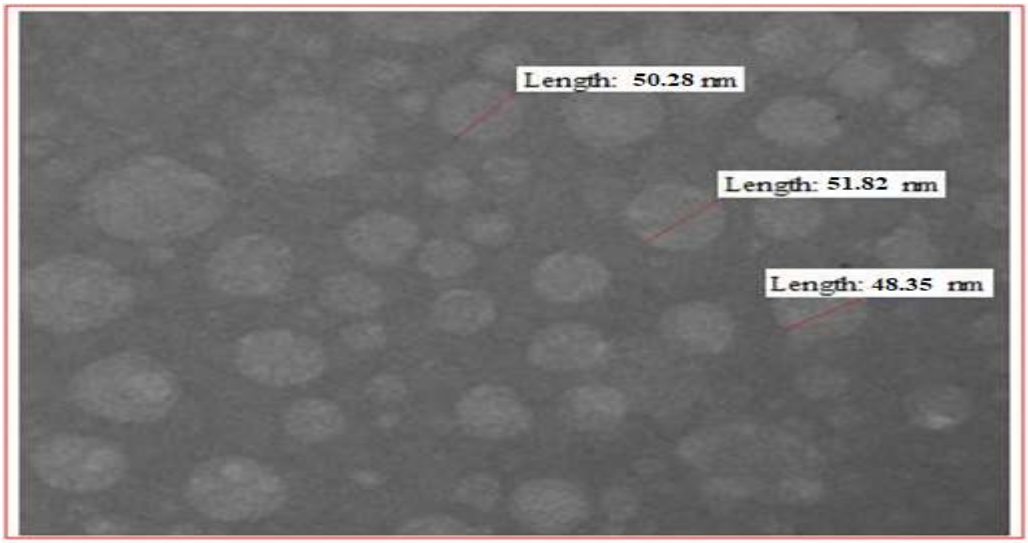

Figure 8: Transmission Electron Microscopic image of Efavirenz nanoparticles obtained using transmission electron microscope

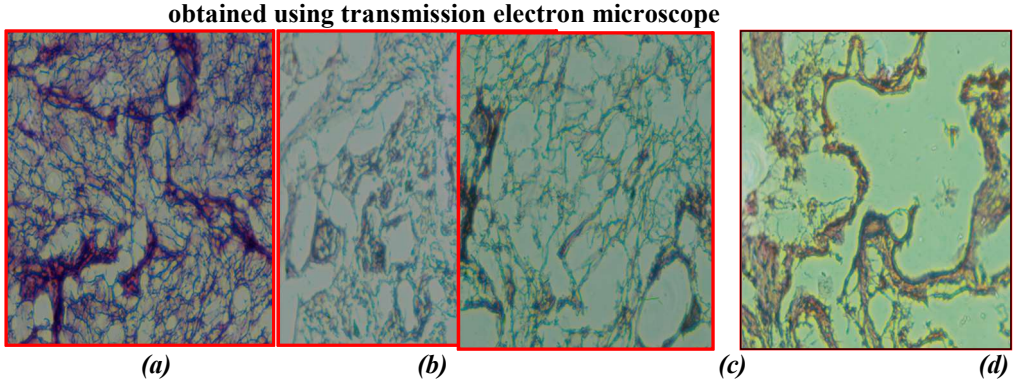

Figure 9: Histopathological conditions of nasal mucosa after treatment with (a) Phosphate buffer saline - PBS pH 6.4 (b) SLN dispersion (c) SLN gel (d) Isopropyl alcohol

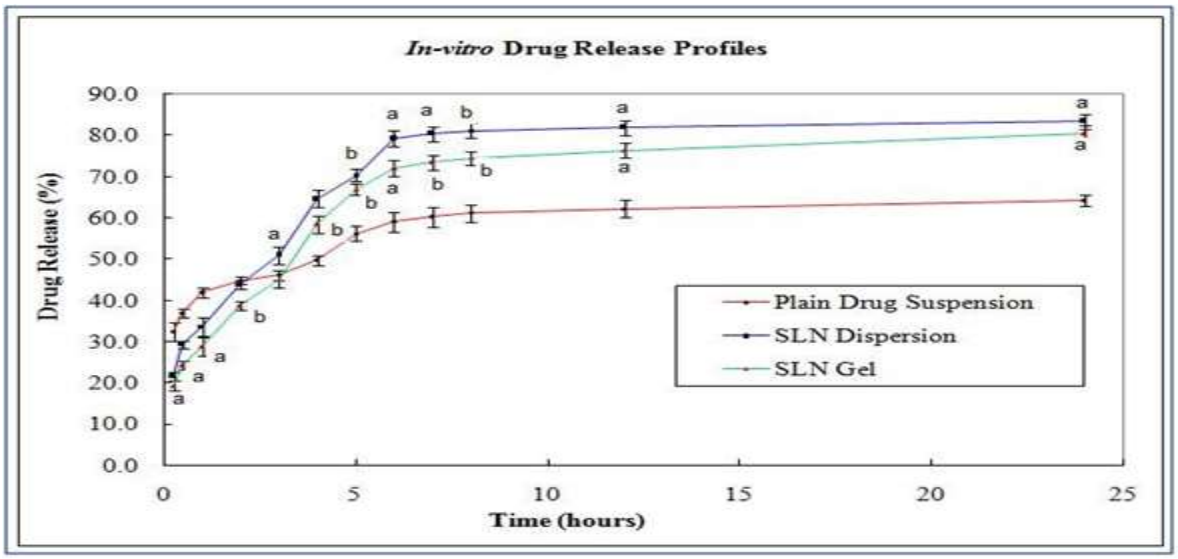

(a): *In-vitro* Drug Release Profile by dialysis-bag method

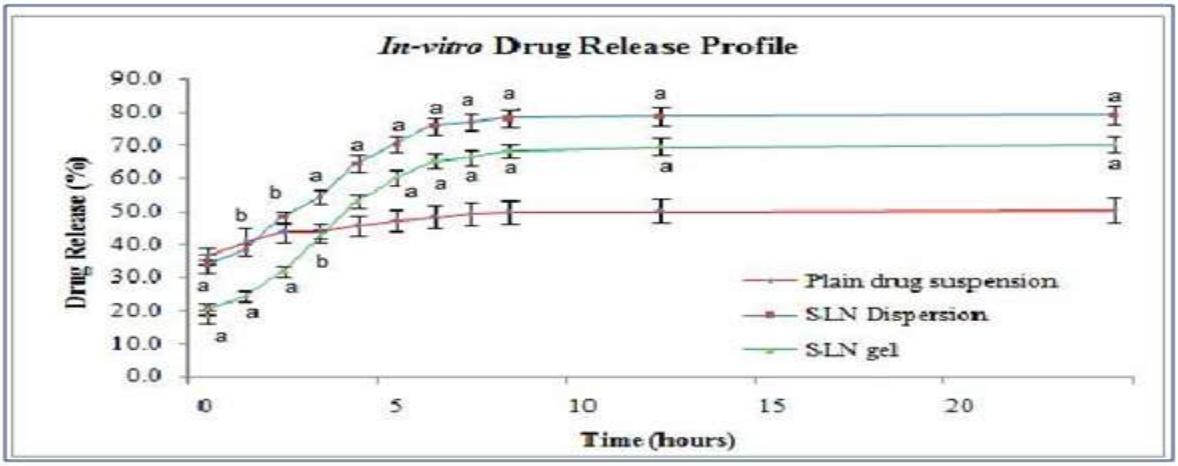

(b): *In-vitro* drug release profile by using Franz-diffusion cell

Figure 10 (a): *In-vitro* Drug Release Profile by dialysis-bag method
(b): *In-vitro* drug release profile by using Franz-diffusion cell
(Different letters indicate statistically significant difference relative to plain drug suspension; a indicate $p < 0.01$ and b indicate $p < 0.05$)

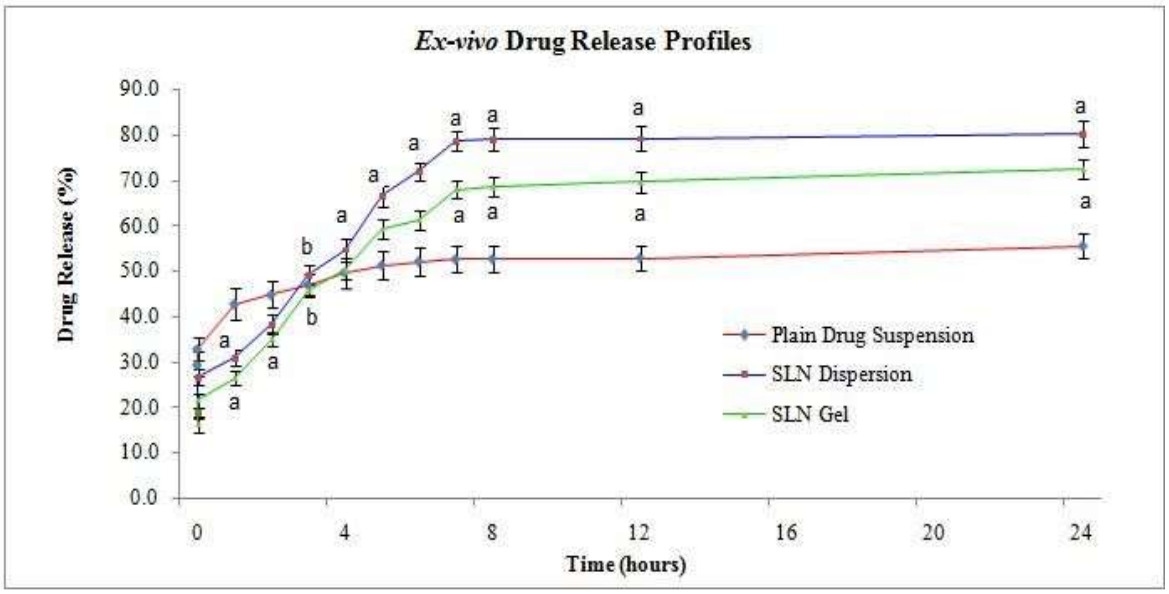

Figure 11: *Ex-vivo* drug release profile by using Franz-diffusion cell (Different letters indicate statistically significant difference relative to PDS; a indicate p <0.01 and b indicate p <0.05)

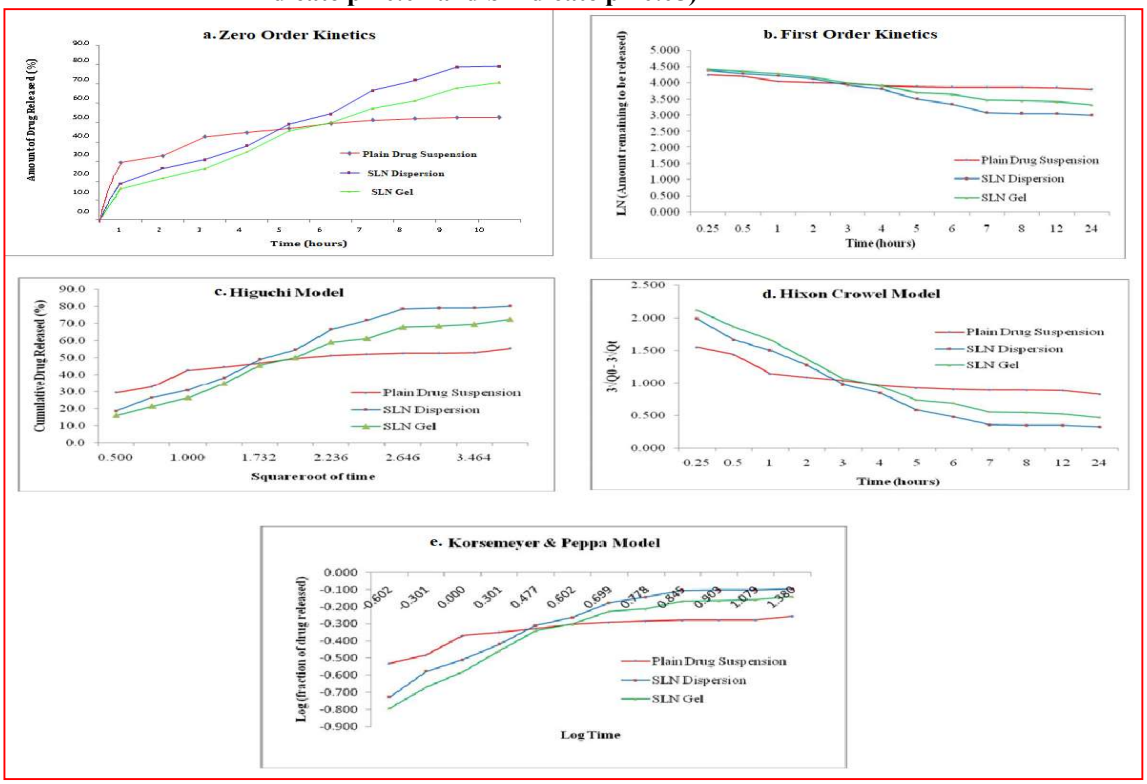

Figure 12 (a): Zero order release kinetics. (b): First order release kinetics. (c): Higuchi Model of release kinetics. (d): Hixon Crowel Model of release kinetics. (e): Korsemeyer and Pepppa's Model of release kinetics

Table 9 (a): Long term stability conditions for the formulation at initial, after 1, 3, 6 and 12 months

Temp (^{0}C)/ RH (%)	Time (months)	Appearance	Particle size* (nm)	PDI*	Zeta Potential* (mV)	Drug content (mg/ml)
5°C ± 3°C	0	Transparent with slight bluish	108.5 ±2.3	0.172 ±0.005	-21.2±1.8	0.25
	1	No significant Change	108.9 ±2.1	0.174 ±0.006	-20.9±1.6	0.25
	3	No significant Change	109.5 ±2.3	0.180 ±0.012	-19.9±2.0	0.25
	6	No significant Change	109.8 ±2.6	0.185 ±0.013	-19.5±1.9	0.25
	12	No significant change	110.2± 2.4	0.195 ±0.015	-19.2±1.8	0.25

*{*Data expressed as mean ± SD (n = 3)}*

Table 9 (b): Accelerated Stability conditions for the formulation at initial, after 1, 3, 6 and 12 months

Temp (^{0}C)/ RH (%)	Time (months)	Appearance	Particle size* (nm)	PDI*	Zeta Potential* (mV)	Drug content (mg/ml)
25°C ± 2°C/60% RH±5% RH	0	Transparent with slight bluish	108.5 ±2.3	0.172 ±0.005	-21.2±1.8	0.25
	1	No significant Change	108.6 ±3.4	0.178 ±0.006	-20.9±2.0	0.25
	3	No significant Change	109.9 ±2.6	0.189 ±0.013	-19.5±1.8	0.25
	6	No significant Change	110.4 ±2.8	0.198 ±0.018	-18.5±1.5	0.25
	12	No significant change	112.5 ±2.7	0.205 ±0.016	-18.2±1.6	0.24